

INFLUENCE OF CROSS-SECTIONAL ELLIPTICITY ON THE DEFORMATION OF A LONG CYLINDRICAL SHELL

Yu. Yu. Abrosov^{*}, V. A. Maximyuk^{*}, and I. S. Chernyshenko^{**}

The computational phenomenon of membrane locking in the variational-difference method is demonstrated. The delayed but stable convergence of numerical calculations of the stress–strain state to the analytical solution is shown. This problem can supplement the collection of so-called pathological tests

Keywords: elliptical cylinder, stress–strain state, membrane locking, variational-difference method

Introduction. Noncircular cylindrical shells are widely used in modern engineering [14]. For example, hollow elliptic sections employed in construction combine the advantages of round and rectangular sections [4]. The cross-sections of fuselages and pressure cockpits of modern aircrafts are made noncircular for reasons of aerodynamics, arrangement of process connections, and internal space efficiency [2, 16]. Of interest is to study the stress–strain state (SSS) [6, 2], stability [4, 16], vibrations [13], and dynamics [11] of such structures and their elements.

The one-dimensional problem of the deformation of a long elliptic cylindrical shell (actually, a ring) under internal pressure has a 150-year history [3, pp. 326–338]. However, the first analytical solutions appeared to be oversimplified. According to the solution found in [3] for a shell under internal pressure, the moments and displacements in two sections by symmetry planes are equal in magnitude (which is a simplification) and opposite in sign (which is correct for high ellipticity).

Timoshenko was the first to obtain (in 1930) correct results, which were published in [12]. He calculated the moments using a table of some coefficients for a number of values of the ellipse aspect ratio. The procedure of determining these coefficients was omitted and is still unknown. In 1965, Roark [15] presented extended tables and formulas to correct for the inhomogeneity of the moment of inertia of the ring (of variable thickness). The further development of analytical and graphical methods was briefly outlined in [7].

The computational phenomenon of membrane locking [10], which is inherent in the problem under consideration due to large deflections under small tension, was demonstrated in [1]. It was shown that the convergence of the numerical calculations of the SSS to the analytical solution [12] is delayed but stable. Of special interest is the occurrence of negative deflections near the major semiaxis at low ellipticity.

1. Problem Statement. Let the midsurface of a closed elliptical cylindrical shell (Fig. 1) be described by the following equation in a Cartesian coordinate system (x, y, z) :

$$F(x, y) = \left(\frac{x}{a}\right)^2 + \left(\frac{y}{b}\right)^2 - 1 = 0, \quad (1)$$

where a and b are the semiaxes of the ellipse.

S. P. Timoshenko Institute of Mechanics, National Academy of Sciences of Ukraine, 3 Nesterova St., Kyiv, Ukraine 03057, e-mail: ^{*}desc@inmech.kiev.ua, ^{**}prikl@inmech.kiev.ua. Translated from *Prikladnaya Mekhanika*, Vol. 52, No. 5, pp. 106–111, September–October, 2016. Original article submitted December 28, 2015.

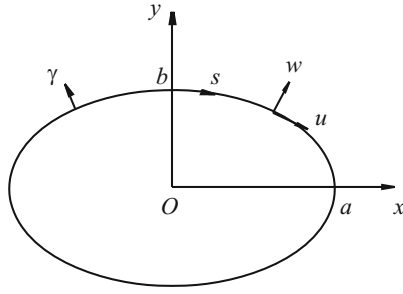


Fig. 1

Let us describe this surface in a curvilinear coordinate system (s, z, γ) , where γ is the normal (to the midsurface) coordinate, and s is the elliptical arc length measured clockwise from the point $(x = 0, y = b)$ (Fig. 1). It is obvious that both coefficients of the first quadratic form in this system are equal to unity ($A_s = A_z = 1$), and the longitudinal curvature is zero.

With the original algorithm of numerical discretization of a plane curve [5], Eq. (1) can be represented in a parametrical form, which can be either as a table or an algorithm:

$$x = x(s), \quad y = y(s). \quad (2)$$

Then the curvature of the ellipse can be determined as follows:

$$k = x'y'' - x''y', \quad (3)$$

where the prime denotes differentiation with respect to the coordinate s .

The SSS in different arbitrary cross-sections of a long shell can be considered the same; therefore, the static problem is one-dimensional. Let a constant uniform internal pressure p cause small transverse displacements and no displacements along the z -axis in an isotropic homogeneous elastic thin shell of constant thickness h . Then the SSS depends on the coordinate s alone. It is clear that the closed shell tends to a nearly circular shape, which causes large deflections near the points at which the symmetry planes cross the ellipse. To calculate the SSS under such conditions, it is reasonable to use the geometrically linear theory of thin shells and a mixed functional simplifying the implementation of the Kirchhoff–Love hypotheses [10].

2. Basic Equations and Problem-Solving Method. The kinematic equations relating the strains of the midsurface and the displacements and angle of rotation are the following [1]:

$$\varepsilon = u' + kw, \quad \kappa = \varphi', \quad (4)$$

where u and w are the components of the displacement vector along the axes (s, γ) , respectively. For the Kirchhoff–Love hypotheses, the angle φ in (4) is determined [10] using Lagrange multipliers and the condition that the transverse-shear strain is equal to zero:

$$\varepsilon_{s\gamma} = \varphi + w' - ku = 0. \quad (5)$$

The tangential strain at an arbitrary point throughout the thickness ($\gamma = \text{const}$) of the shell is defined by the following formula disregarding the change in the metric over the thickness:

$$e = \varepsilon + \gamma\kappa. \quad (6)$$

In a long shell, there are transverse,

$$\sigma_s = Ee / (1 - \nu^2) \quad (7)$$

and longitudinal, $\sigma_z = \nu\sigma_s$, stresses, where E and ν are the elastic modulus and Poisson's ration of an isotropic material.

Stresses (7) are replaced by the thickness-average internal force and moment:

TABLE 1

K	\tilde{s}	\tilde{w}	σ^+ , MPa	σ^0 , MPa	σ^- , MPa	M , N
641	0	2.20	87.88	0.5794	-86.72	1455
	1	-1.01	-109.4	0.6081	110.6	-1833
1281	0	2.36	93.03	0.5273	-91.97	1541
	1	-1.10	-124.0	0.8922	125.7	-2080
2561	0	2.41	94.47	0.5127	-93.45	1566
	1	-1.12	-128.0	0.9724	130.0	-2150
5121	0	2.42	94.85	0.5088	-93.84	1572
	1	-1.13	-129.1	0.9931	131.1	-2168
10241	0	2.42	94.96	0.5077	-93.94	1574
	1	-1.13	-129.3	0.9981	131.3	-2171
[12]	0	—	94.85	0.5	-93.85	1572.5
	1	—	-129.5	1.0	131.5	-2175

$$T = \frac{Eh}{1-\nu^2} \varepsilon, \quad M = \frac{Eh^3}{12(1-\nu^2)} \kappa. \quad (8)$$

For numerical purposes, we will use variational principles and a mixed functional [10]:

$$\Pi(u, w, \varphi, T_{sy}^f) = \frac{1}{2} \iint_{\Omega} (T\varepsilon + M\kappa - 2pw) d\Omega + \iint_{\Omega} T_{sy}^f \varepsilon_{sy} d\Omega. \quad (9)$$

This functional is the sum of the strain energy of the shell and an additional term implementing the geometrical part (5) of the Kirchhoff–Love hypotheses by the Lagrange multiplier (T_{sy}^f) method. It depends on four varied functions: two displacements, angle of rotation, and force T_{sy}^f , which has the physical meaning of shearing force. The advantages of such a functional are outlined in [10].

Note that the superscript in (9) is indicative of the difference between the force formula and the force function and is of methodological importance for the formulation of the boundary conditions and the construction of the algorithm.

The stationarity condition for the functional $\delta\Pi = 0$ leads to the natural static boundary conditions. In the case of symmetry, the principal kinematic conditions are the following [10]:

$$u = 0, \quad \varphi = 0, \quad T_{sy}^f = 0. \quad (10)$$

To determine the stationary values of functional (9), we will use the variational-difference method (VDM), which leads to a system of linear algebraic governing equations with symmetric matrix [10].

3. Analysis of the Numerical Results. Let us determine the SSS of a shell with the following geometrical parameters [1]: $h = 0.01$ m, $a = 1$ m, $b = 0.5$ m. The shell is made of steel with $E = 210$ GPa and $\nu = 0.3$. The load $p = 10$ kPa. Since the

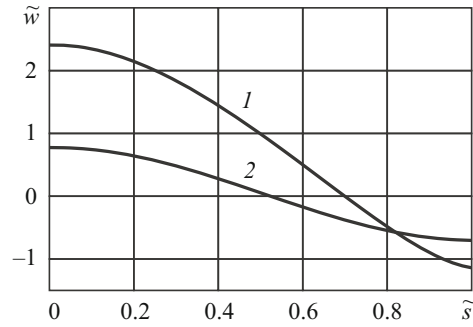


Fig. 2

problem is symmetric about the planes $x = 0$ and $y = 0$ (Fig. 1), we will consider the domain $s \in [0, s_k]$, where $s_k = 1.211$ m is a quarter of the ellipse perimeter, which is calculated by applying the numerical discretization algorithm [5] mentioned above to curve (1). The same algorithm is used to partition the ellipse arc by K equally spaced nodal points. The differentiation in (3) is carried out numerically using difference formulas.

The practical convergence of the SSS calculation [1] with increase in the number K of nodes is demonstrated by Table 1, which summarizes the dimensionless deflections ($\tilde{w} = w/h$), stresses on the outside (σ^+), middle (σ^0), and inside (σ^-) surfaces of the shell, and the moments at the points $\tilde{s} = s/s_k = 0$ (minor semiaxis) and $\tilde{s} = 1$ (major semiaxis).

The last two rows in Table 1 include the exact values of the stresses $\sigma^0(0) = pb/h$ and $\sigma^0(s_k) = pa/h$, the moments $M(0) = 0.629pb^2$ and $M(s_k) = -0.870pb^2$, which include the tabulated coefficients (from [12]) for $b/a = 0.5$, and the stresses $\sigma^+ = \sigma^0 + 6M/h^2$ and $\sigma^- = \sigma^0 - 6M/h^2$ calculated by (6) and (8), respectively, using the previous values (σ^0, M).

Table 1 demonstrates the delayed, yet stable convergence (with mesh refinement) of the VDM calculation of the SSS to the analytical solution [12]. The maximum values of the deflections and the stresses or moments coincide to two significant digits at $K = 2561$, while the membrane stresses σ^0 in the mid-surface coincide somewhat later, at $K = 5121$. At $K < 321$, the fictitious stiffness of the shell is so high that the calculated moments reverse sign near the major semiaxis. Such unwanted numerical effects are due to large deflections under small tension and are called membrane locking or degeneration [10].

Figure 2 shows the distribution of the deflection \tilde{w} over the cross-section \tilde{s} for $b/a = 0.5$ (curve 1) and $b/a = 0.9$ (curve 2). As the ellipticity decreases substantially, the difference between the deflections near the major and minor semi-axes decreases insignificantly. It can be seen that the elliptic shell subject to internal pressure tends to circular shape, causing negative deflections near the major semiaxis.

Of special interest is the occurrence of negative deflections near the major semiaxis at low ellipticity. How the cross-sectional ellipticity affects the strain state of the shell is demonstrated by Table 2, which shows the distribution of the deflection \tilde{w} over the cross-section \tilde{s} for $b/a = 0.9, \dots, 0.99999$. The last row in Table 2 represents a quarter of the ellipse perimeter (s_k/h).

The ellipticity was decreased to one-tenth of the initial seemingly insignificant value $b/a = 0.9$. It appeared that the deflections in the entire cross-section are positive at the third step of decrease in the aspect ratio. This fact indicates that $b/a \sim 0.99995$ is the critical value above which the deflection near the major semiaxis is negative, which is supported by the results in the next-to-last column in Table 2. The deflection near the major semiaxis is positive and three orders of magnitude less than that near the minor semiaxis.

If the cylinder is circular ($b/a = 1$), then $\frac{w}{h} = \frac{a^2}{h^2} (1-\nu^2) \frac{p}{E} \approx 4.33 \cdot 10^{-4}$, $s_k/h = \pi a/2h \approx 157.0796$.

It can be seen from Fig. 2 and Table 2 that the region of negative deflections changes nonmonotonically with decrease in ellipticity. It, first, somewhat increases (Fig. 2) and, then, decreases to disappear (Table 2).

Conclusions. The phenomenon of membrane locking in the VDM based on a mixed functional in which the geometrical part of the Kirchhoff–Love hypotheses is implemented using the Lagrange multiplier method has been demonstrated. It has been shown that the convergence of the numerical calculation of the SSS to the analytical solution is delayed but stable. The effect of sign reversal of the deflection at seemingly insignificant ellipticity has been numerically discovered.

TABLE 2

\tilde{s}	b/a				
	0.9	0.99	0.9999	0.99995	0.99999
0	$7.85 \cdot 10^{-1}$	$8.62 \cdot 10^{-2}$	$1.30 \cdot 10^{-3}$	$8.66 \cdot 10^{-4}$	$5.20 \cdot 10^{-4}$
0.1	$7.51 \cdot 10^{-1}$	$8.20 \cdot 10^{-2}$	$1.26 \cdot 10^{-3}$	$8.45 \cdot 10^{-4}$	$5.16 \cdot 10^{-4}$
0.2	$6.53 \cdot 10^{-1}$	$7.00 \cdot 10^{-2}$	$1.13 \cdot 10^{-3}$	$7.83 \cdot 10^{-4}$	$5.03 \cdot 10^{-4}$
0.3	$4.98 \cdot 10^{-1}$	$5.12 \cdot 10^{-2}$	$9.42 \cdot 10^{-4}$	$6.88 \cdot 10^{-4}$	$4.84 \cdot 10^{-4}$
0.4	$2.99 \cdot 10^{-1}$	$2.76 \cdot 10^{-2}$	$7.01 \cdot 10^{-4}$	$5.67 \cdot 10^{-4}$	$4.60 \cdot 10^{-4}$
0.5	$7.43 \cdot 10^{-2}$	$1.24 \cdot 10^{-3}$	$4.33 \cdot 10^{-4}$	$4.33 \cdot 10^{-4}$	$4.33 \cdot 10^{-4}$
0.6	$-1.57 \cdot 10^{-1}$	$-2.51 \cdot 10^{-2}$	$1.66 \cdot 10^{-4}$	$3.00 \cdot 10^{-4}$	$4.07 \cdot 10^{-4}$
0.7	$-3.71 \cdot 10^{-1}$	$-4.90 \cdot 10^{-2}$	$-7.53 \cdot 10^{-5}$	$1.79 \cdot 10^{-4}$	$3.82 \cdot 10^{-4}$
0.8	$-5.45 \cdot 10^{-1}$	$-6.80 \cdot 10^{-2}$	$-2.67 \cdot 10^{-4}$	$8.32 \cdot 10^{-5}$	$3.63 \cdot 10^{-4}$
0.9	$-6.59 \cdot 10^{-1}$	$-8.02 \cdot 10^{-2}$	$-3.90 \cdot 10^{-4}$	$2.18 \cdot 10^{-5}$	$3.51 \cdot 10^{-4}$
1	$-6.98 \cdot 10^{-1}$	$-8.44 \cdot 10^{-2}$	$-4.32 \cdot 10^{-4}$	$5.86 \cdot 10^{-7}$	$3.47 \cdot 10^{-4}$
s_k/h	149.3290	156.2952	157.0718	157.0757	157.0788

This problem can supplement the collection of so-called pathological tests [8]. In the context of the locking phenomenon, the two-dimensional deformation of a cylindrical shell with fixed ends is a simpler problem because the supports at the ends reduce the deflections. The effect of cross-sectional ellipticity is expected to be stronger in flexible cylindrical shells with holes [9]. It is clear that convergence can be improved by using mixed functionals in which the tangential strain is additionally varied.

REFERENCES

1. Yu. Yu. Abrosova, V. A. Maksimiyuk, and V. S. Tarasyuk, "Deformation of a long thin elliptical cylindrical shell," *Visn. Zaporiz'kogo Nats. Univ., Fiz.-Mat. Nauky*, No. 2, 5–10 (2015).
2. A. Boule, M. Dube, and F. P. Gosselin, "Parametric study of an elliptic fuselage made of a sandwich composite structure," *Mech. Res. Comm.*, **69**, 129–135 (2015).
3. J. A. C. H. Bresse, *Cours de Mecanique Appliquee. Premiere Partie. Resistance des Materiaux et Stabilitie des Constructions*, Deuxieme Edition, Gauthier-Villars, Paris (1866).
4. T. M. Chan, L. Gardner, and K. N. Law, "Structural design of elliptical hollow sections: a review," *Proc. Inst. Civil Engrs.: Struct. Build.*, **163**, No. 6, 391–402 (2010).
5. I. S. Chernyshenko and V. A. Maximiyuk, "On the stress-strain state of toroidal shells of elliptical cross section formed from nonlinear elastic orthotropic materials," *Int. Appl. Mech.*, **36**, No. 1, 90–97 (2000).
6. Ya. M. Grigorenko and L. S. Rozhok, "Applying discrete Fourier series to solve problems of the stress state of hollow noncircular cylinders," *Int. Appl. Mech.*, **50**, No. 2, 105–127 (2014).

7. M. Holland, "Pressurized member with elliptic median line: effect of radial thickness function," *J. Mech. Eng. Sci.*, **18**, No. 5, 245–253 (1976).
8. Rao K. Mallikarjuna and U. Shrinivasa, "A set of pathological tests to validate new finite elements," *Sadhana*, **26**, 549–590 (2001).
9. V. A. Maximyuk, E. A. Storozhuk, and I. S. Chernyshenko, "Stress–strain state of flexible orthotropic cylindrical shells with a reinforced circular hole," *Int. Appl. Mech.*, **51**, No. 4, 425–433 (2015).
10. V. A. Maximyuk, E. A. Storozhuk, and I. S. Chernyshenko, "Variational finite-difference methods in linear and nonlinear problems of the deformation of metallic and composite shells (review)," *Int. Appl. Mech.*, **48**, No. 6 613–687 (2012).
11. V. F. Meish and M. P. Kopenach, "Nonstationary dynamics of longitudinally reinforced elliptic cylindrical shells," *Int. Appl. Mech.*, **50**, No. 6, 677–682 (2014).
12. S. P. Timoshenko, *Strength of Materials. Part II, Advanced Theory and Problems*, 2nd ed., D. Van Nostrand Company, New York (1941).
13. F. Tornabene, N. Fantuzzi, M. Baccocchi, and R. Dimitri, "Free vibrations of composite oval and elliptic cylinders by the generalized differential quadrature method," *Thin Walled Struct.*, **97**, 114–129 (2015).
14. K. P. Soldatos, "Mechanics of cylindrical shells with non-circular cross-section: a survey," *Appl. Mech. Rev.*, **52**, No. 8, 237–274 (1999).
15. W. C. Young and R. G. Budynas, *Roark's Formulas for Stress and Strain*, 7th ed., McGraw-Hill, New York (2002).
16. L. P. Zheleznov, V. V. Kabanov, and D. V. Boiko, "Nonlinear deformation and stability of oval cylindrical shells under pure bending and internal pressure," *J. Appl. Mech. Tech. Phys.*, **47**, No. 3, 406–411 (2006).